

# Excess-noise dependence on intracavity aperture shape

G. P. Karman, G. S. McDonald, J. P. Woerdman, and G. H. C. New

In lasers with nonorthogonal eigenmodes the excess-noise factor  $K$  can be large, especially in unstable-cavity lasers with hard-edged intracavity apertures. To the best of our knowledge, we report the first detailed study of the dependence of  $K$  on aperture shape. Calculations and measurements of  $K$  for unstable-cavity lasers with variable-size apertures of triangular, square, pentagonal, hexagonal, octagonal, and rhomboid symmetries are summarized. It is shown that both the magnitude of  $K$  and its resonant behavior strongly depend on aperture shape and that many aspects of this dependence can be explained in terms of one-dimensional resonance lengths. © 1999 Optical Society of America

OCIS codes: 140.3460, 050.1220, 050.1940, 270.2500, 270.3430.

## 1. Introduction

Unstable-cavity lasers have recently attracted much attention because of the interesting properties of their eigenmodes. For example, the eigenmodes form a nonorthogonal set<sup>1,2</sup> and have been shown to have fractal structure.<sup>3</sup> Mode nonorthogonality has profound consequences for the quantum-limited linewidth  $\Delta\nu$  of these lasers. For standard lasers—with orthogonal eigenmodes—this linewidth is given by the usual Schawlow–Townes expression,<sup>4</sup> but for lasers with nonorthogonal eigenmodes this expression must be multiplied by a factor  $K$ , the so-called excess-noise factor.<sup>1,2</sup> In terms of a mode profile  $U(s)$  and its adjoint  $V(s)$ ,  $K$  can be expressed as<sup>5</sup>

$$K = \frac{1}{\left| \int_{-\infty}^{\infty} U(s)V(s)ds \right|^2}, \quad (1)$$

---

When this research was performed, G. P. Karman, G. S. McDonald, and J. P. Woerdman (qo@rulhm1.leidenuniv.nl) were with the Huygens Laboratory, Leiden University, P.O. Box 9504, 2300 RA Leiden, The Netherlands. G. P. Karman (gerwin.karman@philips.com) is now with the Philips Research Laboratories, Prof. Holstlaan 4, 5656 AA Eindhoven, The Netherlands. G. S. McDonald (g.mcdonald@salford.ac.uk) was also with the Blackett Laboratory, Imperial College, but is now with the Department of Physics, University of Salford, Salford M5 4WT, UK. G. H. C. New (g.new@ic.ac.uk) is with the Blackett Laboratory, Imperial College, London SW7 2BZ, UK.

Received 1 July 1999; revised manuscript received 1 July 1999.  
0003-6935/99/336874-05\$15.00/0

© 1999 Optical Society of America

where  $s$  is transverse space. The magnitude of  $K$  can be large, especially in hard-edged unstable-cavity lasers.<sup>5–9</sup> Its value depends on the detailed field distribution of the eigenmode, which in turn depends on the geometry of the cavity. In particular, variation of the size of the intracavity aperture results in  $K$  passing through resonances that are due to mode crossings; near degeneracy of nonorthogonal modes can lead to large cancellations in the denominator of Eq. (1).<sup>5,9</sup> Although it is known that  $K$  can depend on aperture shape,<sup>7,10</sup> only lasers with square and circular apertures have previously been the subject of detailed investigation. This is because circular and square geometries can be handled by one-dimensional (1-D) diffraction theory, dramatically simplifying analyses of the eigenmodes.<sup>5,7,11</sup>

Only one paper exists in which other shapes were investigated,<sup>10</sup> but this concerned a laser with a longitudinally distributed aperture in the form of a capillary with, for example, a triangular cross section. In that case variation of the aperture size was not possible and, therefore, since  $K$  shows strongly resonant behavior as a function of aperture size, this work did not lead to further insight into the effect of aperture shape on the  $K$  factor. Also, theoretical analysis was not possible in that case; theory is available only for conventional shapes of a hard-edged aperture. Thus, the extent to which a truly two-dimensional (2-D) transverse geometry influences  $K$  has remained an open question.

Here, we report what we believe is the first theoretical and experimental investigations of  $K$  factors arising in lasers with fully 2-D (discrete) variable-size aperturing. We have chosen a range of aperture shapes to examine the role of fundamental symmetries in determining  $K$ . Regular polygonal and

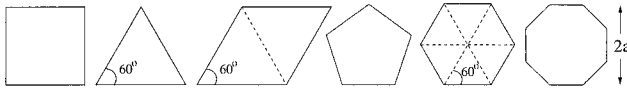


Fig. 1. All the aperture shapes are regular polygons, except for the rhombus. The dashed lines show how some of the shapes can be constructed from equilateral triangles.

rhomboid apertures were employed (see Fig. 1) and  $K$  as a function of aperture shape and size is presented. The method we developed that permits such apertures to be constructed easily is also described. Finally, we discuss the extent to which results can be explained by considering dominant 1-D resonance lengths.

## 2. Experimental Arrangement

Unstable cavities are characterized by two variables: the linear round-trip magnification  $M$  and the equivalent Fresnel number  $N_{\text{eq}}$ . This latter quantity depends on aperture dimension through

$$N_{\text{eq}} = \frac{M^2 - 1}{2M} \frac{a^2}{\lambda B}, \quad (2)$$

where  $2a$  is the aperture size (as indicated in Fig. 1) and  $B$  is the second element in an  $ABCD$ -matrix description of the cavity, i.e., a generalized cavity length.<sup>12</sup> Although  $N_{\text{eq}}$  has only a clear physical definition in the case of a 1-D strip (or 2-D cylindrical) resonator, we define an analogous quantity for the aperture shapes of Fig. 1 to permit comparisons and to keep our notation consistent.

To measure  $K$  factors experimentally, we used a miniature He-Xe laser operating on  $\lambda = 3.51 \mu\text{m}$ . The setup is shown in Fig. 2 and is similar to that of Refs. 13 and 14. The technical details are as follows: cavity length  $L = 7.8 \text{ cm}$ , radii of curvature of  $M_{1,2}$  are  $+21 \text{ cm}$  (gold, reflectivity  $R = 99\%$ ) and  $-30 \text{ cm}$  (dielectrically coated,  $R = 80\%$ ), respectively, yielding  $M = 1.3$ . To determine the quantum-limited linewidth  $\Delta\nu$  we used the polarization-rotation technique<sup>13</sup>; by applying a magnetic field over the cavity the  $\sigma_+/\sigma_-$  degeneracy is lifted and the resulting beat signal is measured after polarizer  $P$  with detector  $D_2$ . This signal is free from technical noise and its Lorentzian spectrum—the fingerprint of quantum noise—yields  $\Delta\nu$ . We also checked that  $\Delta\nu$  was proportional to inverse output power (measured by  $D_1$ ). The proportionality constant, together with a measurement

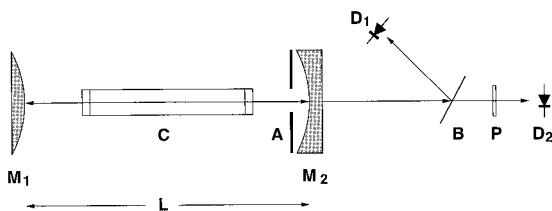


Fig. 2. Experimental setup:  $M_{1,2}$ , mirrors; C, capillary; B, beam splitter;  $D_{1,2}$ , detectors; P, polarizer; A, aperture (positioned within 1 mm of  $M_2$ ).

of the cavity loss rate, gives enough information to calculate  $K$ . More details of this procedure are given in Refs. 13 and 14.

Given that  $K$  exhibits resonances as  $N_{\text{eq}}$  varies, it is not sufficient to compare differently shaped apertures of fixed size. Variable-size apertures are thus required. The method of construction we developed is particularly suited to polygon shapes. We modified commercial iris diaphragms by removing a number of blades from each diaphragm, retaining three blades to form a triangle, five for a pentagon, and so forth. In this way a range of variably sized apertures was obtained. However, for polygons with a large number of corner points, such as the octagon, it was difficult to obtain apertures with good symmetry.

## 3. Experimental and Theoretical Results

Because of the finite diameter of capillary  $C$  (5 mm), we were limited to small Fresnel numbers  $N_{\text{eq}} < 1.7$ . However, this was still sufficient to observe resonant behavior of  $K$ , allowing for a sensitive test of the theory. First we compared theoretical mode profiles with intensity profiles that we measured by using an 8-bit IR camera (type IQ-325 from FLIR Systems, Inc.). These showed good agreement. Of course, measurements of  $K$  factors provide a much more sensitive—and interesting—test of the theory since, near a resonance,  $K$  is particularly sensitive to the profiles of the crossing modes.<sup>5,9</sup> The observed values of  $K$  versus  $N_{\text{eq}}$  for the different aperture shapes are shown in Fig. 3.

The theoretical curves in Fig. 3 show data from numerical simulations of each of the experimental configurations. An iterative power method was used to determine the profile of the lowest-loss mode at each  $N_{\text{eq}}$ .  $K$  factors were then calculated directly from the field profiles of these modes. To increase the accuracy of our results, we employed nonorthogonal grids for the discretization of the transverse plane.<sup>15</sup> Grid angles were chosen that most closely matched the symmetries of the apertures (for example, in the case of a triangular aperture we used a  $60^\circ$  grid). This permitted  $256 \times 256$  transverse points to be sufficient for most  $N_{\text{eq}}$  values up to 2. A denser discretization of  $512 \times 512$  points was used for higher values of  $N_{\text{eq}}$ . As a criterion for convergence, we insisted that the  $K$  value of the field distribution remain constant to within 1% during a number of consecutive transits. A more detailed account of the computational technique, and its application to  $K$  factors, will be reported in a future publication.

In view of the quite distinct means of determining the experimental and theoretical data, Fig. 3 demonstrates good agreement between measured and computed dependencies of  $K$  factor on  $N_{\text{eq}}$ . The main discrepancy is in the resonance for the triangle, which is slightly displaced in comparison with theory. This may be due to the sensitive dependence of peak position on aperture dimension or perhaps is due to slight asymmetries in the triangular apertures. It is interesting to note that, in contrast with the other shapes, there are two resonances for the rhombus.

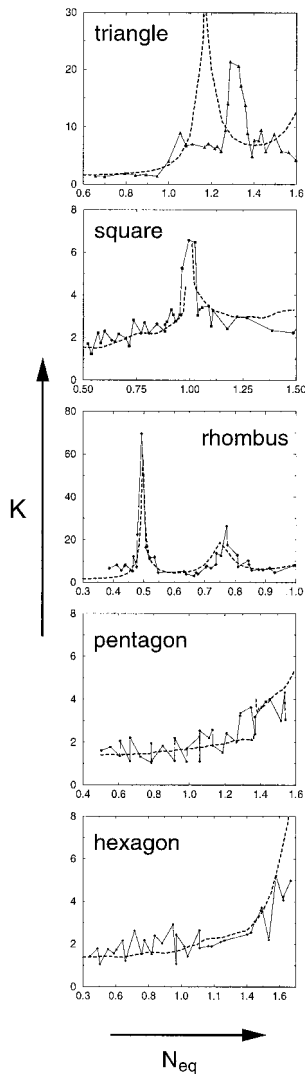


Fig. 3. Measured and calculated  $K$ -factor dependencies on equivalent Fresnel numbers for different aperture shapes. Points with solid curves represent experimental results; the dashed curves represent theory.

#### 4. Discussion

The good agreement with experiment for small  $N_{eq}$  gives us confidence that the iterative numerical code gives accurate results and that it can be used to draw more general conclusions about the dependence of  $K$  on aperture shape and size. To facilitate a comparison of results for the different shapes, we plot the calculated curves together in Fig. 4, showing an overview of predicted dependencies in the range  $N_{eq} = 0-5$ . The exact height of the resonances is determined by the precise value of  $N_{eq}$  that one chooses, and it can be difficult to determine because, near each peak, the number of round trips needed for convergence of the calculation tends to become very large ( $>10^4$ ). Available computation time thus limits the resolution of each peak. Figure 4 shows that significant differences arise when one varies the aperture shape. The underlying trend (not accounting for

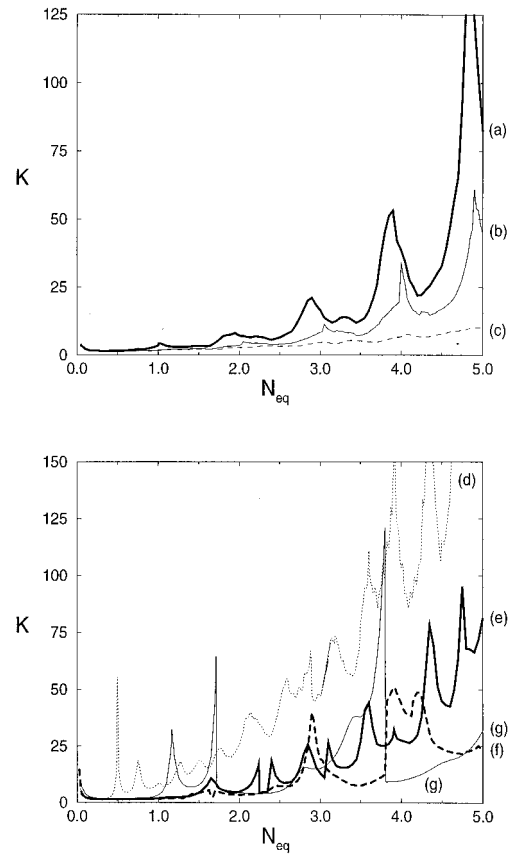


Fig. 4. Calculated  $K$  factors for different aperture shapes as a function of  $N_{eq}$  at  $M = 1.3$ : (a) square, (b) octagon, (c) circle, (d) rhombus, (e) hexagon, (f) pentagon, (g) triangle.

specific resonances) is that a circular aperture minimizes  $K$ , whereas rhomboid aperturing maximizes it. The difference between these two extremes is approximately an order of magnitude. Note that the octagon curve lies between the hexagon and the circle, an assuring result, because it indicates that, when the shape converges toward a circle, the  $K$  factor also converges toward the  $K$  factor of the circle.

The complex structure of the curves invites physical interpretation. This task is potentially difficult because each curve has discontinuities (mode crossings) and is actually composed of sections of several distinct curves that are not shown. Despite this, we find that some progress can be made by associating  $K$ -factor peaks with 1-D resonance lengths. Our reference datum is the dependence of  $K$  on  $N_{eq}$  for the lowest-loss modes of 1-D strip resonators. In this case, the peak heights depend on  $M$  but their positions are approximately invariant with respect to this parameter; peaks reside near, and just below, integer values of  $N_{eq}$ .<sup>12,16</sup>

The  $K$  factor for a square aperture is precisely the (mathematical) square of the corresponding 1-D result,<sup>5,7</sup> thus peaks arise at the same positions in the two cases. In geometric terms, peaks of the square curve can be associated with the simultaneous resonance of two orthogonal 1-D lengths (labeled  $L_0$  in

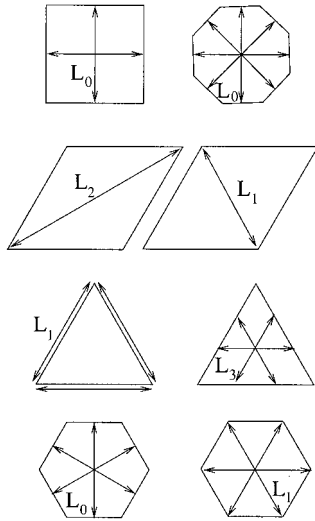


Fig. 5. One-dimensional lengths used in the interpretation of the maxima of  $K$ -factor curves.

Fig. 5). Next, we note that an octagonal aperture can be considered as having four  $L_0$  resonances, as it consists of two identical squares that overlap at an angle of  $45^\circ$ . The top frame of Fig. 4 shows that positions of the peaks of the octagon curve are in broad agreement with those of the square curve. However, an increased number of simultaneous resonances (which are not all mutually orthogonal) does not imply higher  $K$  factors; they appear to combine in a manner that averages out cancellations in the denominator of Eq. (1). The curve for the circular aperture (representing an infinite number of such resonances) confirms this trend and has  $K$  peaks that are barely visible.

The most striking feature of the bottom frame of Fig. 4 is the rhombus curve, which has many closely spaced peaks of relatively high  $K$  factor. These features can be explained in terms of the rhombus diagonals; diffractive edge waves appear to resolve along these directions to give 1-D resonances. The long diagonal ( $L_2$  of Fig. 5) is twice the length of  $L_0$ . A Fresnel number based on this dimension is four times larger than that given by Eq. (2) and, inasmuch as  $K$  generally increases with Fresnel number, this could imply prominent peaks. Denoting 1-D slit resonances as  $N_{\text{eq}} = S^{(j)}$ , where  $j = 1, 2, 3, \dots$  (in order of increasing  $N_{\text{eq}}$ ),  $L_2$  resonances should appear at  $N_{\text{eq}} = R^{(j)} = S^{(j)}(L_0/L_2)^2$ . The first eight peaks of the rhombus curve that are visible correspond to  $R^{(j)}$  with  $j = 2, 3, \dots, 9$ . This suggests an additional peak at  $N_{\text{eq}} \approx 0.25$ . Indeed, closer examination reveals a low amplitude peak at precisely this value and confirms a predictive capacity of 1-D resonance theory.

At low  $N_{\text{eq}}$ , the rhombus curve is thus different from the others because of the sheer magnitude of the long diagonal  $L_2$ . However, the height of  $S^{(j)}$  peaks does not increase monotonically with  $j$ ;  $S^{(9)}$  is the peak at which this trend abruptly stops for  $M = 1.3$ .

Consequently, the dominant resonance length switches to one that is shorter and can exploit the stronger resonances at lower  $j$ . The natural candidate is the second largest internal dimension of the rhombus (the short diagonal,  $L_1$ ). Inasmuch as  $L_1 < L_2$ , the peaks at higher  $N_{\text{eq}}$  are more widely spaced.

The triangular aperture has the fewest sides and the smallest overall size of the cases shown in Fig. 1. Resonance lengths are thus generally shorter but are more difficult to identify. However, inasmuch as there are only three sides, one could suspect  $K$ -factor peaks of a magnitude comparable with those of square and rhombus geometries. The triangular curve does indeed exhibit relatively few resonances (characteristic of shorter resonance lengths), and its main features are of quite high amplitude. Five local maxima can be identified that correlate with lengths  $L_1$  and  $L_3$  (and perhaps also  $L_0$ ) of Fig. 5. The rationale behind identifying  $L_3$  is that it represents an average internal dimension, which could plausibly give rise to approximately symmetric maxima. On the other hand,  $L_1$  represents an extreme case (the largest internal length of the triangle) and could lead to sharp falls in  $K$  as  $N_{\text{eq}}$  varies.

The final shape highlighted in Fig. 5 is the hexagon. As with square and octagonal apertures,  $L_0$  resonances are likely given that this shape also consists of the intersection of 1-D strips. However, even though  $K$  peaks are found in the vicinity of  $N_{\text{eq}} = 3, 4, \text{ and } 5$ , the majority of resonances appear to be of the  $L_1$  type ( $j = 3, 4, 5, 6, \text{ and } 7$  are all present).  $L_1$  is the distance between opposite corners and the largest internal dimension. It is also the length of the shorter rhombus diagonal and, above  $N_{\text{eq}} = 3$ , peaks of the two curves are aligned. As in the triangular case, the pentagon data are difficult to interpret. An odd number of aperture sides seems to result in less well-defined resonances and generally broader  $K$  peaks (such as in the pentagon curve near  $N_{\text{eq}} = 2.9$ ). Nevertheless, resonance lengths can still be identified for the peaks that appear.

## 5. Conclusions

In conclusion, we have calculated and measured the lowest-loss eigenmodes and the corresponding  $K$  factors of a low  $N_{\text{eq}}$  unstable-cavity laser with polygon- and rhombus-shaped intracavity apertures. We have shown that the transverse symmetry of the resonator plays a significant role. Theoretically evaluated  $K$  factors show good agreement with experimental results. In particular, resonant behavior of  $K$  is confirmed independently from both approaches. We found that circular apertures tend to give the lowest  $K$  values and rhomboid aperturing the highest; the difference between the two being a factor of approximately 10. Other aperture shapes tend to result in intermediate  $K$  values. Increasing the number of sides of the polygon, yielded  $K$  factors that converge toward the  $K$  factor of the circle. Finally, it was shown that most features of the dependence of  $K$  on aperture shape can be explained in terms of one-dimensional resonance lengths. More

detailed investigations, which include studies of mode patterns, additional aperture shapes, and a wider range of  $N_{eq}$  and  $M$ , are under way.

The authors acknowledge G. Nelissen for his experimental assistance and J. Post for designing and constructing the variable-size apertures. This study is part of the research program of the Foundation for Fundamental Research on Matter. We also acknowledge support from the European Union, under European Strategic Programme for R&D in Information Technology contract 20029; Advanced Quantum Information Research and Training and Mobility of Researchers contract ERB4061PL95-1021; Microlasers and Cavity Quantum Electrodynamics, and funds from the UK Engineering and Physical Sciences Research Council, grant GR/L90583.

## References

1. K. Petermann, "Calculated spontaneous emission factor for double-heterostructure injection lasers with gain-induced waveguiding," *IEEE J. Quantum Electron.* **QE-15**, 566–570 (1979).
2. A. E. Siegman, "Excess spontaneous emission in non-Hermitian optical systems. I. Laser amplifiers," *Phys. Rev. A* **39**, 1253–1263 (1989); "Excess spontaneous emission in non-Hermitian optical systems. II. Laser oscillators," *Phys. Rev. A* **39**, 1264–1268 (1989).
3. G. P. Karman and J. P. Woerdman, "Fractal structure of eigenmodes of unstable-cavity lasers," *Opt. Lett.* **23**, 1909–1911 (1998).
4. A. L. Schawlow and C. H. Townes, "Infrared and optical masers," *Phys. Rev.* **112**, 1940–1949 (1958).
5. G. H. C. New, "The origin of excess noise," *J. Mod. Opt.* **42**, 799–810 (1995).
6. A. E. Siegman, "Lasers without photons—or should it be lasers with too many photons?," *Appl. Phys. B* **60**, 247–257 (1995).
7. M. A. Rippin and G. H. C. New, "Excess-noise factors in circular unstable resonators," *J. Mod. Opt.* **43**, 993–1008 (1996).
8. Y. J. Cheng, C. G. Fanning, and A. E. Siegman, "Experimental observation of a large excess quantum noise factor in the linewidth of a laser oscillator having nonorthogonal modes," *Phys. Rev. Lett.* **77**, 627–630 (1996).
9. M. A. van Eijkelenborg, A. M. Lindberg, M. S. Thijssen, and J. P. Woerdman, "Resonance of quantum noise in an unstable-cavity laser," *Phys. Rev. Lett.* **77**, 4314–4317 (1996).
10. M. A. van Eijkelenborg, A. M. Lindberg, M. S. Thijssen, and J. P. Woerdman, "Influence of transverse resonator geometry on excess noise," *Opt. Commun.* **137**, 303–307 (1997).
11. W. H. Southwell, "Unstable-resonator-mode derivation using virtual-source theory," *J. Opt. Soc. Am. A* **3(11)**, 1885–1891 (1986).
12. A. E. Siegman, *Lasers* (University Science, Mill Valley, Calif., 1986).
13. A. M. Lindberg, M. A. van Eijkelenborg, and J. P. Woerdman, "Measuring the quantum-limited linewidth of a laser using the Zeeman effect," *IEEE J. Quantum Electron.* **33**, 1767–1773 (1997).
14. G. P. Karman, A. M. Lindberg, and J. P. Woerdman, "Observed factorization of excess quantum noise that is due to both polarization and spatial mode nonorthogonality," *Opt. Lett.* **23**, 1698–1700 (1998).
15. G. S. McDonald and W. J. Firth, "Spatial grid symmetries and reduced models in the simulation of beam counterpropagation in a nonlinear medium," *J. Mod. Opt.* **40**, 23–32 (1993).
16. G. S. McDonald, G. H. C. New, and J. P. Woerdman, "Excess noise in low Fresnel number unstable resonators," *Opt. Commun.* **164**, 285–295 (1998).